Vol 15 No 2, February 2006
1009-1963/2006/15(02)/0412-10
Chinese Physics
© 2006 Chin. Phys. Soc.
and IOP Publishing Ltd

Propagation of acoustic wave in viscoelastic medium permeated with air bubbles*

Liang Bin(梁 彬), Zhu Zhe-Min(朱哲民), and Cheng Jian-Chun(程建春)†

Laboratory of Modern Acoustics and Institute of Acoustics, Nanjing University, Nanjing 210093, China

(Received 8 August 2005; revised manuscript received 23 September 2005)

Based on the modification of the radial pulsation equation of an individual bubble, an effective medium method (EMM) is presented for studying propagation of linear and nonlinear longitudinal acoustic waves in viscoelastic medium permeated with air bubbles. A classical theory developed previously by Gaunaurd (Gaunaurd GC and Überall H, *J. Acoust. Soc. Am.*, 1978; 63: 1699–1711) is employed to verify the EMM under linear approximation by comparing the dynamic (i.e. frequency-dependent) effective parameters, and an excellent agreement is obtained. The propagation of longitudinal waves is hereby studied in detail. The results illustrate that the nonlinear pulsation of bubbles serves as the source of second harmonic wave and the sound energy has the tendency to be transferred to second harmonic wave. Therefore the sound attenuation and acoustic nonlinearity of the viscoelastic matrix are remarkably enhanced due to the system's resonance induced by the existence of bubbles.

Keywords: acoustic wave, viscoelastic medium, bubble, nonlinearity
PACC: 4335, 4325, 6240

1. Introduction

Attempts to study the sound propagation in inhomogeneous materials go back many decades,[1−11] and research in this field is still active[12−15] due to the potential applications to a large variety of important situations, such as underwater sound absorption. Gaunaurd *et al*[1−3] have presented an effective medium theory (EMT) based on the resonance scattering theory and compared it comprehensively with a multiple scattering theory (MST) of Waterman and Truell.[4] The results showed that[5] the effective properties of porous viscoelastic medium predicted by these two methods agree well. Both the EMT and the MST are appropriate for acoustic propagation under linear approximation. However, the strong nonlinear effects have been observed in experiments for a solid medium permeated with air bubbles. Ostrovsky[6,7] presented a nonlinear theory based on the Rayleigh–Plesset-like equation describing nonlinear radial pulsation of an individual bubble. But only the static solutions are obtained by neglecting the radiation loss and the acoustic properties are predicted at low frequencies.

In this paper, based on the modification of the Rayleigh–Plesset-like equation by considering the friction damping and radiation loss, we present an effective medium method (EMM) to investigate the longitudinal wave in porous viscoelastic medium permeated with air bubbles. The dynamic effective parameters for both linear and nonlinear acoustic waves are numerically calculated, and the results illustrate that the modification is necessary for the Rayleigh–Plesset-like equation in the viscoelastic medium. The EMM is verified by comparing it comprehensively with the classical Gaunaurd's EMT under linear approximation for different matrix materials, such as neoprene, polyurethane and silicone. By using the EMM, the propagation of longitudinal waves in porous viscoelastic medium is investigated in detail, and the results show that the sound attenuation and acoustic nonlinearity of viscoelastic medium are dramatically increased due to the system's resonance induced by the existence of bubbles.

2. Theory

*Project supported by the Excellent Youth Science Foundation of China (Grant No 10125417) and the State Key Development Program of Basic Research (Grant No 51315).
†E-mail: jccheng@nju.edu.cn

2.1. Longitudinal wave equation in porous viscoelastic medium

For the one-dimensional case, the longitudinal wave equation in solids may be written as follows:

$$\rho_0 \frac{\partial^2 \varepsilon}{\partial t^2} = \frac{\partial^2 \sigma}{\partial x^2}, \tag{1}$$

where ρ_0 is the mass density, ε is the longitudinal strain, and σ is the corresponding stress.

One considers a plane longitudinal wave in a medium permeated with air bubbles with small porosity. For simplicity, we assume that all bubbles have the uniform radius r_0. If the bubbles are small compared to the wavelength, and the amount of bubbles per wavelength is great enough, this medium may be regarded as an "effective" medium, which is homogeneous and can be described by "effective" parameters, and the continual approach may be employed to investigate the wave propagation in it.

Under these circumstances the acoustic wave equation remains unchanged as Eq.(1), whereas the stress–strain relation is affected by the additional deformation of bubbles. On condition of small porosity, it can be proved[8] that the multiple scattering effects can be neglected and the bubbles can be treated independently. Taking into consideration of the additional deformation of bubbles, the longitudinal deformation of a thin layer of porous medium of thickness $\mathrm{d}x$ is given as below:

$$\mathrm{d}u = \frac{\sigma \mathrm{d}x}{\lambda + 2\mu} + V_\mathrm{c}\mathrm{d}x, \tag{2}$$

where λ and μ are the Lamé coefficients, u is the longitudinal displacement of particle, $V_\mathrm{c} = NU$ is the change of porosity, N is the bubble amount per unit volume, U is volume perturbation of an individual bubble. The porosity is defined as $\Phi = 4\pi N r_0^3/3$.

By rewriting Eq.(2), the stress–strain relation for longitudinal deformation may now be expressed in terms of the "averaged" Hooke's law, i.e.

$$\sigma = (\lambda + 2\mu)(\varepsilon - NU).$$

Then we readily deduce the acoustic equation for longitudinal wave in porous medium as follows:

$$\frac{\partial^2 \sigma}{\partial t^2} - \frac{\lambda + 2\mu}{\rho_0}\frac{\partial^2 \sigma}{\partial x^2} = -N(\lambda + 2\mu)\frac{\partial^2 U}{\partial t^2}. \tag{3}$$

On condition that the matrix material is viscoelastic, the Lamé coefficients may be rewritten as

$$\lambda = \lambda_\mathrm{e} + \mathrm{j}\lambda_\mathrm{v}\frac{\partial}{\partial t}, \quad \mu = \mu_\mathrm{e} + \mathrm{j}\mu_\mathrm{v}\frac{\partial}{\partial t},$$

where λ_e and μ_e are the elastic Lamé coefficients, λ_v and μ_v are lossy factors given by Kelvin–Voigt viscoelastic model. In the following we shall adopt the assumption that the dilatational viscosity is negligible, i.e. λ_v=0, as is usually done in the case of rubberlike media.[16]

2.2. Dynamic equation of an individual bubble in viscoelastic medium

In order to solve Eq.(3), the relationship between U and σ is needed. Ostrovsky[6,7] proposed a Rayleigh–Plesset-like equation describing the radial pulsation of an individual bubble in elastic matrix as follows:

$$\ddot{U} + \omega_0^2 U - r_0/c_l \dddot{U} = GU^2 + q(2U\ddot{U} + \dot{U}^2) + e\sigma, \tag{4}$$

where

$$\omega_0 = \sqrt{\omega_1^2 + \omega_2^2},$$
$$\omega_1 = \sqrt{4\mu_\mathrm{e}/\rho_0 r_0^2},$$
$$\omega_2 = \sqrt{3\rho_\mathrm{g} c_\mathrm{g}^2/\rho_0 r_0^2},$$

ρ_g and c_g are the mass density and sound velocity of gas in the bubble, respectively, $c_l = \sqrt{(\lambda_\mathrm{e} + 2\mu_\mathrm{e})/\rho_0}$ is the speed of longitudinal wave in the elastic material of matrix. The parameters G, q and e are given as

$$G = (9 + 2\beta)\, q\omega_0^2/2, \quad q = 1/(8\pi r_0^3), \quad e = 4\pi r_0/\rho_0,$$

where β is another constant such that $0 < \beta \leq 1$, or in its more simplified version with β=1.[7]

Ostrovsky[7] considered only acoustic waves at low frequencies, which lies far below the bubble resonance frequency. Accordingly all terms with time derivatives in Eq.(4) are neglected and static solutions are eventually obtained.

However, in order to obtain the dynamic effective properties of porous viscoelastic medium, every term with time derivative in Eq.(4) should be retained to obtain the dynamic solutions. Particularly, if the elastic matrix is weakly compressible, for which the inequality $\lambda_\mathrm{e} \gg \mu_\mathrm{e}$ is fulfilled, the term $-r_0/c_l \dddot{U}$ responsible for the radiation of scattered waves from the bubble should be retained.[6] On the other hand, the friction damping of bubble pulsation will occur due to the existence of viscoelasticity in the case of lossy matrix. This effect may be taken into account by adding a corresponding term responsible for it to

the left-hand part in Eq.(4). According to the general form of the equation describing a forced resonance system, the term of friction damping is assumed to the equal to $\nu\dot{U}$, where ν is an undetermined coefficient. Adding the term of friction damping $\nu\dot{U}$ and retaining the term of radiation $-r_0/c_l\dddot{U}$ yield the modified radial pulsation equation of an individual bubble in viscoelastic matrix as follows:

$$\ddot{U}+\omega_0^2U+\nu\dot{U}-r_0/c_l\dddot{U}=GU^2+q(2U\ddot{U}+\dot{U}^2)+e\sigma. \quad (5)$$

Note that a substitution of μ_e in Eq.(4) with μ is virtually equivalent to the introduction of $\nu\dot{U}$, the following equality is supposed to be satisfied:

$$\frac{4\mu_e}{\rho_0 r_0^2}U \to \frac{4\mu}{\rho_0 r_0^2}U \to \frac{4\mu_e}{\rho_0 r_0^2}U+\frac{4\mu_\nu}{\rho_0 r_0^2}\frac{\partial}{\partial t}U=\omega_0^2U+\nu\dot{U}.$$

Then one obtains

$$\nu=\frac{4\mu_v}{\rho_0 r_0^2}.$$

It is apparent that Eq.(4) is a nonlinear equation. Up to the second order approximation, a potential solution has the form

$$\sigma(x,t)\approx\sigma^{(1)}+\sigma^{(2)}, \quad U(t)\approx U^{(0)}+U^{(1)}+U^{(2)}, \quad (6)$$

where

$$\sigma^{(1)}=\sigma_1\exp(\mathrm{j}\omega t)+\text{c.c.}, \quad \sigma^{(2)}=\sigma_2\exp(\mathrm{j}2\omega t)+\text{c.c.},$$

$$U^{(1)}=U_1\exp(\mathrm{j}\omega t)+\text{c.c.}, \quad U^{(2)}=U_2\exp(\mathrm{j}2\omega t)+\text{c.c.}.$$

In the preceding definitions, $\sigma_1=\sigma_1(x)$ and $\sigma_2=\sigma_2(x)$ represent the linear and nonlinear longitudinal waves, respectively; $U^{(0)}$ is the change in the time-average volume due to the nonlinear response of the bubble, $U_1=U_1(\omega)$ is the amplitude of the linear pulsation, $U_2=U_2(\omega)$ is the amplitude of the nonlinear response.

Substituting Eq.(6) into Eq.(5) and equating the quantities with the same-order magnitude yield

$$U^{(0)}=\frac{2(G-q\omega^2)e^2\sigma_1\sigma_1^*}{\chi_1^2\omega^4\omega_0^2},$$
$$U^{(1)}=-\frac{e}{\omega^2\chi_1}\sigma_1\exp(\mathrm{j}\omega t+\mathrm{j}\phi)+\text{c.c.}, \quad (7)$$

$$U^{(2)}=-\frac{1}{4\omega^2\chi_2}[D\sigma_1^2\exp(2\mathrm{j}\omega t+2\mathrm{j}\phi+\mathrm{j}\varphi)+e\sigma_2\exp(2\mathrm{j}\omega t+\mathrm{j}\varphi)]+\text{c.c.}, \quad (8)$$

where $\sigma_1^*=\sigma_1^*(x,\omega)$; the parameters D, χ_1, χ_2, ϕ and φ are given as

$$D=\frac{e^2(G-3q\omega^2)}{\chi_1^2\omega^4},$$
$$\chi_1=\left[(1-\Omega^2)^2+(k_0r_0+1/Q)^2\right]^{1/2},$$
$$\chi_2=\left\{(1-\Omega^2/4)^2+[2k_0r_0+1/(2Q)]^2\right\}^{1/2},$$
$$\phi=\tan^{-1}\left(\frac{1/Q+k_0r_0}{1-\Omega^2}\right),$$
$$\varphi=\tan^{-1}\left[\frac{1/(2Q)+2k_0r_0}{1-\Omega^2/4}\right],$$

where $\Omega=\omega_0/\omega$, $k_0=\omega/c_l$ is the longitudinal wavenumber in homogeneous elastic material of matrix, and $Q=\omega/\nu$ is the quality factor.

Substituting Eqs.(6–8) into Eq.(3), one obtains the linear and nonlinear longitudinal wave equations describing the propagations of fundamental and second harmonic waves in porous viscoelastic medium as follows:

$$\frac{\mathrm{d}^2\sigma_1}{\mathrm{d}x^2}+(\Lambda_1^2+\Delta_1^2)\sigma_1=0, \quad (9)$$
$$\frac{\mathrm{d}^2\sigma_2}{\mathrm{d}x^2}+(\Lambda_2^2+\Delta_2^2)\sigma_2=-\Gamma\sigma_1^2, \quad (10)$$

where Λ_i accounts for the viscoelasticity of homogeneous medium, Δ_i stems from influence on the stress-strain relationship exerted by the additional deformation of bubbles; i=1, 2 refer to fundamental and second harmonic waves, respectively. And Γ represents the transfer of energy from fundamental to second harmonic waves. The parameters $\Lambda_{1,2}$, $\Delta_{1,2}$ and Γ are given in the Appendix.

2.3. Fundamental and second harmonic waves

The effective wavenumbers are defined as complex numbers and can be expressed in terms of real effective wave speeds and attenuations as follows:

$$\tilde{k}_1\equiv\sqrt{\Lambda_1^2+\Delta_1^2}=\mathrm{Re}\tilde{k}_1-\mathrm{j}\mathrm{Im}\tilde{k}_1=\omega/c_1-\mathrm{j}\alpha_1,$$
$$\tilde{k}_2\equiv\sqrt{\Lambda_2^2+\Delta_2^2}=\mathrm{Re}\tilde{k}_2-\mathrm{j}\mathrm{Im}\tilde{k}_2=2\omega/c_2-\mathrm{j}\alpha_2,$$

where c_1 and c_2 are the (real) effective sound speeds of the fundamental and second harmonic waves, respectively; α_1 and α_2 are the effective attenuations of these waves.

Letting $\sigma_1(x,\omega)=\sigma_{1A}\exp(-\mathrm{j}\tilde{k}_1x)$, from Eq.(9) one readily obtains the expression of α_1 and c_1 as follows:

$$c_1=\omega\left(\frac{-B+\sqrt{B^2+4A}}{2}\right)^{-1/2}, \quad (11a)$$

$$\alpha_1 = Ac_1/\omega, \tag{11b}$$

where the parameters of A, B are given in the Appendix.

Notice that the solution of Eq.(10) should consist of a general solution σ_{2g} and a special solution σ_{2s}, i.e., $\sigma_2 = \sigma_{2g} + \sigma_{2s}$. The potential solutions of σ_{2g} and σ_{2s} have the forms

$$\sigma_{2g} = \sigma_{2g0}\exp(-\tilde{k}_2 x) + \text{c.c.}, \tag{12a}$$

$$\sigma_{2s} = \sigma_{2s0}\exp(-2\tilde{k}_1 x) + \text{c.c.}. \tag{12b}$$

Substituting Eq.(12a) into the homogeneous form of Eq.(10) yields

$$c_2 = \omega\left(\frac{-F + \sqrt{F^2 + 4E}}{2}\right)^{-1/2}, \tag{13a}$$

$$\alpha_2 = Ec_2/\omega, \tag{13b}$$

$$\sigma_{2s0} = H\sigma_{1A}^2, \tag{14}$$

where the parameters F, E, and H are given in the Appendix.

Using the boundary condition that the second harmonic wave should be zero at the beginning, viz., $\sigma_2|_{x=0} = \sigma_{2g}|_{x=0} + \sigma_{2s}|_{x=0} = 0$, one can readily determine from Eq.(12),

$$\sigma_{2g0} = -\sigma_{2s0}. \tag{15}$$

Substituting Eqs.(14) and (15) into Eq.(10), we eventually obtain the second harmonic wave as follows:

$$\sigma^{(2)} = \sigma_{1A}^2\exp(-\alpha_2 x)\chi_3\cos(2\omega t - \tilde{k}_2 x + \theta), \tag{16}$$

where the parameters of χ_3 and θ are given in the Appendix.

With the purpose of guaranteeing the convergence of the approximation solution, the amplitude of the second harmonic wave is supposed to be much less than that of the fundamental wave: i.e., the following inequality should be fulfilled:

$$\frac{\sigma_{1A}^2\exp(-\alpha_2 x)\chi_3}{\sigma_{1A}\exp(-\alpha_1 x)} = \sigma_{1A}\chi_3\exp\left[(\alpha_1 - \alpha_2)x\right] \ll 1.$$

As observed from the expression of $U^{(1)}$ given by Eq.(7), the linear pulsation of bubble reaches its maximum if $1 - \Omega^2 = 0$, i.e., $\omega = \omega_0$, and bubble resonance occurs, which is the reason that ω_0 is defined as the bubble resonance frequency. Analogously, the nonlinear resonance occurs at $\omega = \omega_0/2$ where the nonlinear response of bubbles reaches its maximum, as seen from Eq.(8).

3. Numerical results

3.1. Influence of friction damping and radiation loss

If one neglects the terms $\nu\dot{U}$ and $-r_0/c_l\dddot{U}$ at the same time, what Eq.(2) describes will be the forced pulsation of a single bubble that is totally undamped, the response of bubble to driving force with finite amplitude will tend to be infinite when resonance occurs, and numerical divergence will occur at resonance frequency. Therefore we will confine our attention to the cases where there exists at least one of these two terms.

Figures 1 and 2 show the dispersion and attenuation curves of porous viscoelastic medium predicted by the EMM for three the cases: (1) the term $\nu\dot{U}$ is neglected (dash-dotted line); (2) the term $-r_0/c_l\dddot{U}$ is neglected (dotted line); and (3) the terms $\nu\dot{U}$ and $-r_0/c_l\dddot{U}$ are retained (solid line). In numerical simulations, all the bubbles have uniform radius r_0=0.1mm, the porosity is Φ=0.1%. The material of matrix is neoprene with the lossy factor μ_v=50P and the mechanical parameters ρ_0=1300kg/m^3, c_l=1400m/s, c_s=94m/s, where c_s is the speed of shear waves in the matrix. In Fig.1 and following figures, the normalized effective sound speeds are defined by c_i/c_l (i=1 and 2) for the fundamental and second harmonic waves, respectively.

It is apparent in Figs.1 and 2 that the basic shapes of the dispersion and attenuation curves of fundamental and second harmonic waves in porous media are very similar, except that the resonances occur at different frequencies. The differences caused by neglecting the friction damping or the radiation loss are negligible at the frequencies far from the bubble resonance frequency, where the resonance effects of bubbles is relatively weak. However, the differences of both the fundamental and second harmonic waves are remarkably enhanced near the resonance frequency, where the resonance effects of bubble are strong and contribute dominantly to the vibrating damping of bubbles.

Therefore, it is necessary to modify the pulsation equation of the bubble so as to guarantee the accuracy of the EMM. In the followings, the EMM based on the modified pulsation equation will be verified by making a comparison between it and the Gaunaurd's EMT.

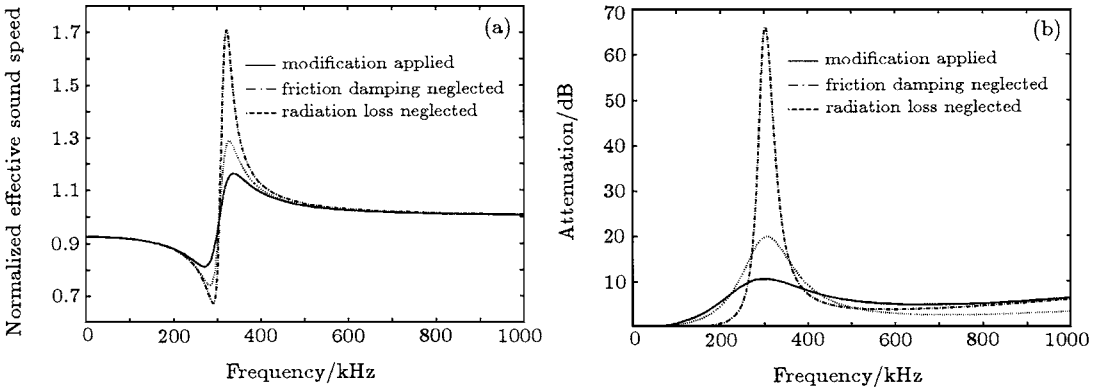


Fig.1. The dispersion (a) and attenuation (b) curves of fundamental wave for three different cases.

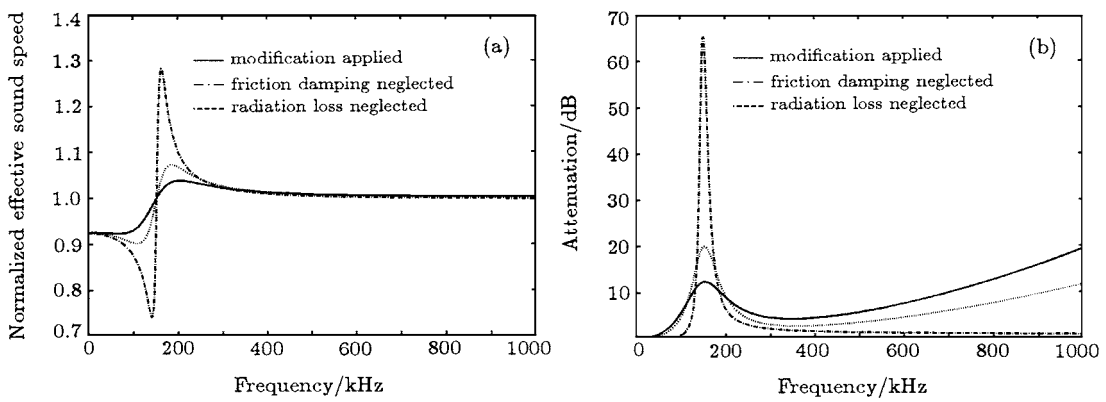


Fig.2. The dispersion (a) and attenuation (b) curves of second harmonic wave for three different cases.

3.2. Fundamental wave

3.2.1. Bubble resonance frequencies

For porous viscoelastic medium, the expressions of resonance frequency of an individual bubble predicted by the EMM and by Gaunaurd's EMT (see Eq.8(a) and 8(b) in Ref.[2]) can be expressed as $\omega_0 = \sqrt{\omega_1^2 + \omega_2^2}$. Here ω_1 corresponds to the Meyer–Brendel–Tamm (MBT) resonance,[9] and ω_2 corresponds to the Minnaert bubble resonance.[2] Neglecting the influence of gas within the bubbles that is comparatively small, the expressions of ω_0 predicted by two methods are exactly identical and is given approximately by $\omega_0 \approx \sqrt{4\mu_e/\rho_0 r_0^2}$.

3.2.2. Dynamic effective parameters

Figure 3 shows the dispersion and attenuation curves of the fundamental wave for three different materials, permeated with same bubbles, predicted by the EMM (solid line) and Gaunaurd's EMT (circles), respectively. The expressions of normalized effective sound speed and attenuation predicted by Gaunaurd's EMT are given by Eqs.(33) and (34) in Ref.[3]. Curves 1, 2 and 3 refer to the materials of matrix: silicone rubber, neoprene, and polyurethane. The bubbles have uniform radius r_0=0.5mm, the porosity is Φ=0.3%. The mechanical parameters are ρ_0=1100kg/m^3, c_l=1700m/s, c_s=200m/s for polyurethane and ρ_0=1000kg/m^3, c_l=1700m/s, c_s=20m/s for silicone rubber, respectively.

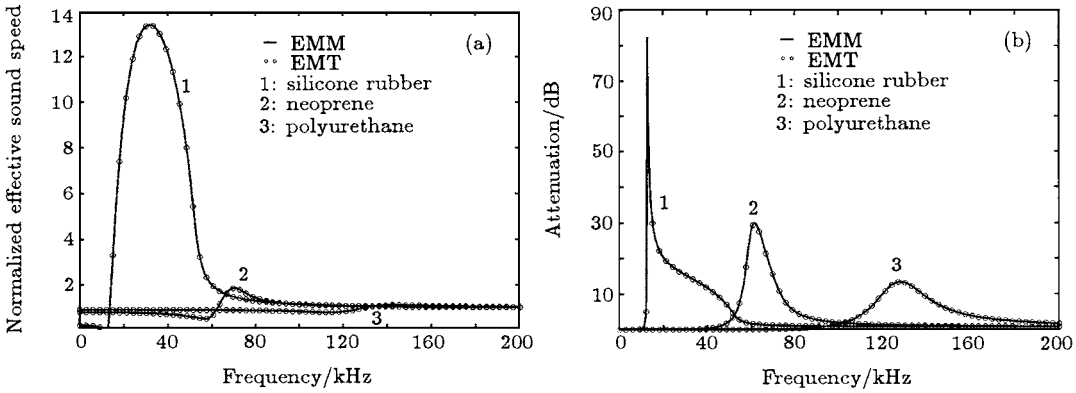


Fig.3. The dispersion (a) and attenuation (b) curves of the fundamental wave for three different porous elastic materials predicted by two methods.

Figure 4 illustrates the dispersion and attenuation curves of the fundamental wave for a porous elastic medium, permeated with three different bubbles: r_0= 0.1 mm and Φ=0.1% (curve 1), r_0=0.1mm and Φ=0.3% (curve 2), r_0=0.5mm and Φ=0.3% (curve 3), predicted by the EMM (solid line) and Gaunaurd's EMT (circles), respectively. Figure 5 displays the dispersion and attenuation curves of the fundamental wave for porous elastic (curve 1) and viscoelastic (curves 2 and 3) materials predicted by the EMM (solid lines) and Gaunaurd's EMT (circles), respectively. Curves 2 and 3 refer to the lossy factors μ_ν=50P and 5P, respectively. The bubbles have uniform radius r_0=0.5mm, the porosity is Φ=0.5%. In Figs. 4 and 5 the material of matrix is silicone rubber.

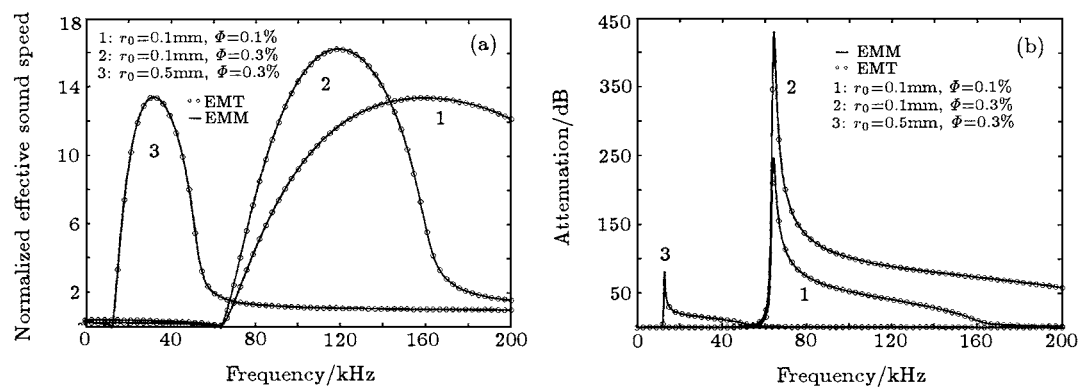


Fig.4. The dispersion (a) and attenuation (b) curves of the fundamental wave for an elastic medium permeated with three different bubbles, predicted by two methods.

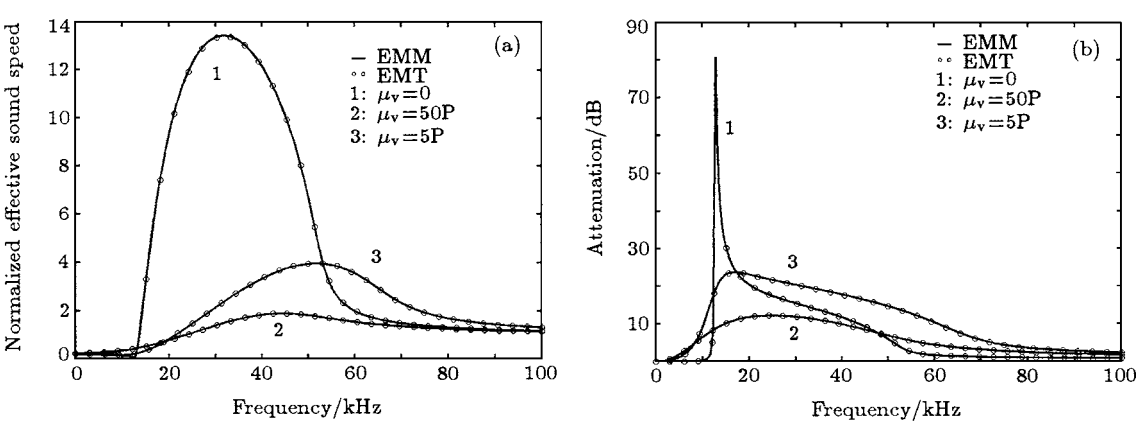


Fig.5. The dispersion (a) and the attenuation (b) curves of the fundamental wave predicted by two methods for porous media assumed to be elastic and viscoelastic.

As shown in Fig.3 to Fig.5, one can see an excellent agreement between the EMM and Gaunaurd's EMT. The shapes of dispersion and attenuation curves for fundamental wave are similar for different cases. The existence of bubbles will introduce the system's resonances which is the dominant mechanism for sound attenuation compared with viscoelasticity of the matrix. The attenuation curves thus display a remarkable attenuation-enhanced effect near the bubble resonance frequency, rather than being linearly proportional to frequency as in homogeneous viscoelastic medium.

It can be easily seen in Fig.3 that the degree of dispersion is more severe for media with smaller shear modulus, which are more compressible. According to the expression of bubble resonance frequency, one has $\omega_0 \sim \sqrt{\mu_e}/r_0$. Hence the resonance frequency can be reduced by decreasing the shear modulus of the matrix or enlarging the bubbles. And the attenuation coefficients may be collectively enhanced as the porosity Φ increases, because the medium includes more bubbles contributing to the attenuation. This can be observed in Figs.3 and 4.

The existence of viscoelasticity of matrix increases the vibration damping of bubbles and reduces the quality factor Q, according to $Q \sim 1/\mu_s$. For longitudinal wave in viscoelastic matrix, therefore, the dispersive curves vary more smoothly and the attenuation curves are lowered in height and take on a broader and flatter shape compared to the case of elastic matrix. This is the typical characters of a resonance system with small quality factor and can be seen in Fig.5.

3.3. Second harmonic wave

Figure 6 displays the sound pressures of the fundamental (curve 1) and second harmonic (curve 2) waves versus distance in porous elastic medium predicted by the EMM. The angular frequency of incident wave equals the bubble resonance frequency, i.e. $\omega = \omega_0$. The material of matrix is silicone rubber and the porosity is Φ=0.1%. In Fig.6 and the following figures, the sound pressure of the incident longitudinal wave is $p_{1A} = 2\sigma_{1A}$=10^4Pa and the bubbles have uniform radius r_0=0.5mm. In the figures, the sound pressure of the second harmonic wave $p_{2A} = |\sigma^{(2)}|$, and $\sigma^{(2)}$is given in Eq.(16).

As illustrated in Fig.6, the behaviours of the fundamental and second harmonic waves in porous medium virtually differ from each other. The fundamental wave always decays exponentially along the propagation direction, whereas the second harmonic wave does not exist initially, then it grows sharply and reaches its maximum within a short propagation distance less than one millimetre, and decreases gradually along the propagation direction. The growing of second harmonic wave represents a continuous accumulation of sound energy, which results from the transfer of sound energy from the fundamental wave. This effect partially accounts for the enhancement of sound attenuation of the fundamental wave. As the propagation distance grows, however, the attenuation of the second harmonic wave becomes predominant in comparison with the effect of energy transfer, thus the second harmonic wave damps with propagation.

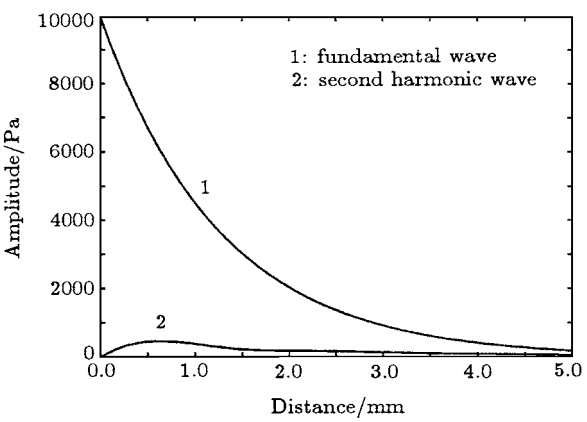


Fig.6. The sound pressures of the fundamental and second harmonic waves versus distance in porous elastic medium (silicone rubber) predicted by the EMM at frequency $\omega = \omega_0$=80kHz.

Note that the nonlinearity of porous viscoelastic medium is considerably strong, although the Mach number is quite small ($\sim 10^{-6}$). Here the Mach number is defined as $M = v_{1A}/c_l$, v_{1A} is the amplitude of particle velocity defined by the relationship $p_{1A} = \rho_0 c_l v_{1A}$. Hence it is apparent that the strong nonlinearity stems chiefly from the "physical" nonlinearity due to the inhomogeneous structure, rather than the "kinematic" nonlinearity which associates with the motion of the particles.[7]

Figure 7 shows the sound pressures of the second harmonic wave versus distance in porous elastic medium for three different frequencies: $\omega = \omega_0$ (curve 1), ω=0.1ω_0 (curve 2) and ω=5ω_0 (curve 3), predicted by the EMM. The material of matrix is silicone rubber and the porosity is Φ=0.1%.

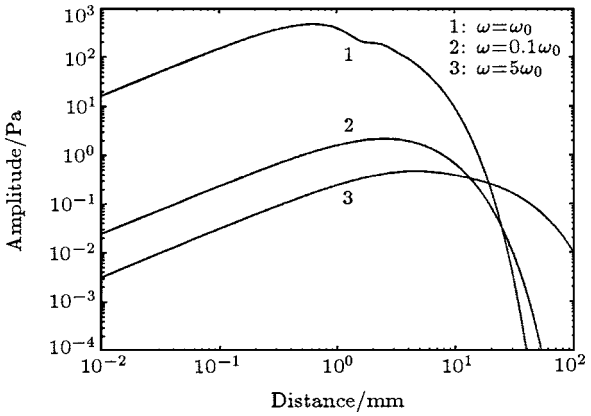


Fig.7. The sound pressures of the second harmonic wave versus distance in porous elastic medium for three different frequencies, predicted by the EMM. The resonance frequency ω_0=80kHz.

It can be observed in Fig.7 that the second harmonic wave is extraordinarily strong near the resonance frequencies, where the bubbles pulsate violently and the nonlinear pulsation of bubbles can act as the source of second harmonic wave. Contrarily, at the frequencies far from the resonance frequencies, the resonance effects of bubbles are comparatively weak and the problem nearly degenerates to the sound propagation in homogeneous viscoelastic medium.

Figure 8 illustrates the sound pressures of the second harmonic wave versus distance in porous elastic medium predicted by the EMM for two different materials: neoprene (curve 1) and silicone rubber (curves 2 and 3). The angular frequencies of incident waves equal the corresponding resonance frequencies of bubbles. Curves 1, 2 and 3 refer to the porosities of bubbles: Φ=0.1%, Φ=0.1% and Φ=1%, respectively.

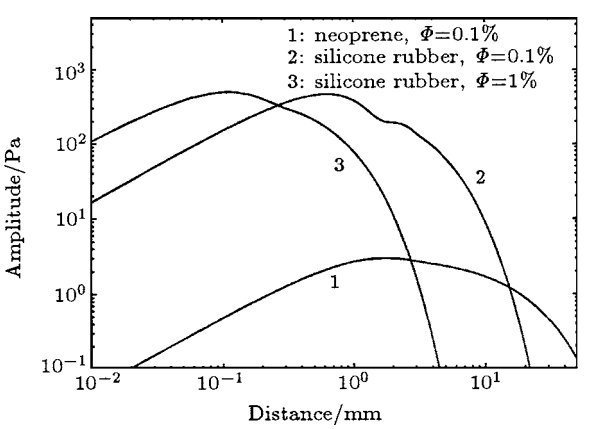


Fig.8. The sound pressures of the second harmonic wave versus distance in porous elastic medium predicted by the EMM for two different materials. The resonance frequencies are ω_0=376kHz and ω_0=80kHz for porous neoprene and silicone rubber, respectively.

In the medium of smaller shear modulus that is more compressible, it is easier for the bubbles to pulsate; the transfer of energy from the fundamental wave and the attenuation of second harmonic wave are notably enhanced, therefore the growth and decay of the second harmonic wave become more abrupt, and the peak value is also enlarged greatly at resonance frequencies. Similarly, the second harmonic wave will be generated and damped more quickly if the porosity of bubbles is increased, due to the larger number of bubbles contributing to the sound attenuation, as shown in Fig.8.

Figure 9 displays the sound pressures of the second harmonic wave at the resonance frequencies versus distance in porous elastic (curve 1) and viscoelastic (curves 2 and 3) materials predicted by the EMM. The material of matrix is silicone rubber. Curves 2 and 3 refer to the lossy factors μ_ν=5P and 50P, respectively.

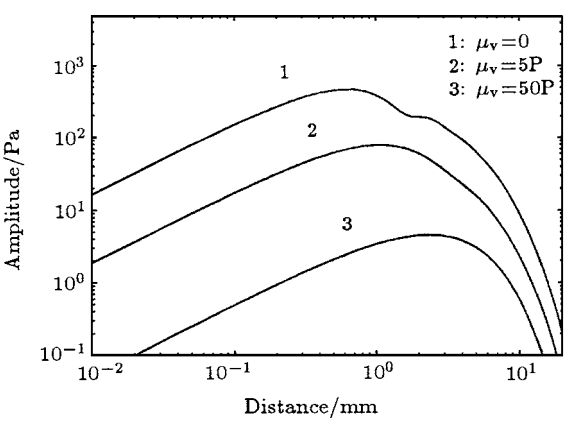


Fig.9. The sound pressures of the second harmonic wave versus distance in porous elastic and viscoelastic materials predicted by the EMM. The resonance frequency ω_0=80kHz.

The viscoelasticity of matrix affects the nonlinear pulsation of bubbles in the same manner as it does to the linear one. The pulsating bubbles have to overcome the effects of friction damping introduced by the viscoelasticity. It becomes more difficult for bubbles to pulsate as the viscoelasticity increases. Therefore, the generation of second harmonic wave is suppressed, which results in a lower peak value and a slower growth of it. This effect of viscoelasticity of matrix on second harmonic wave is obviously illustrated in Fig.9.

4. Conclusion

On the basis of the modified Rayleigh–Plesset-like equation, we present an EMM for studying the propagation of the linear and nonlinear longitudinal waves in viscoelastic medium permeated with air bubbles. We can conclude that: (1) it is necessary to modify the Rayleigh–Plesset-like equation of the bubble so as to guarantee the accuracy of EMM, especially at frequencies near the resonance frequency; (2) the validity of EMM is verified by comparing it with Gaunaurd's EMT under linear approximation for different materials of matrix; (3) the nonlinear pulsation of bubbles becomes the source of the second harmonic wave near the resonance frequency, and the sound energy has the tendency to be transferred to second harmonic wave. Hence the sound attenuation and acoustic nonlinearity of viscoelastic medium is dramatically increased due to the system's resonance induced by the existence of bubbles

Appendix

The parameters of $\Lambda_{1,2}$, $\Delta_{1,2}$ and Γ used in Eqs.(9) and (10) are given as follows:

$$\Lambda_1^2 = \rho_0\omega^2/[(\lambda_e + 2\mu_e) + j(\lambda_v + 2\mu_v)\omega],$$

$$\Lambda_2^2 = 4\rho_0\omega^2/[(\lambda_e + 2\mu_e) + j2(\lambda_v + 2\mu_v)\omega],$$

$$\Delta_1^2 = -\frac{\rho_0 Ne}{\chi_1}\exp(j\phi),$$

$$\Delta_2^2 = -\frac{\rho_0 Ne}{\chi_2}\exp(j\varphi),$$

$$\Gamma = -\frac{\rho_0 N}{\chi_2}D\left[\exp(2j\phi + 2j\varphi)\right].$$

The parameters of A and B used in Eq. (11) are given as follows:

$$B = \frac{Ne\rho_0}{\chi_1}\left(\cos\phi - \frac{\lambda_v + 2\mu_v}{\lambda_e + 2\mu_e}\omega\sin\phi\right) + \frac{\lambda_v + 2\mu_v}{\lambda_e + 2\mu_e}2\omega A - \frac{\omega^2\rho_0}{\lambda_e + 2\mu_e},$$

$$A = \frac{Ne\rho_0}{2\chi_1}\sin\phi + \frac{(\lambda_v + 2\mu_v)\omega^3\rho_0}{2(\lambda_e + 2\mu_e)^2 + 2(\lambda_v + 2\mu_v)^2\omega^2}.$$

The parameters of E,F and H used in Eqs.(13) and (14) are given as follows:

$$F = \frac{Ne\rho_0}{\chi_2}\left(\cos\varphi - \frac{\lambda_v + 2\mu_v}{\lambda_e + 2\mu_e}2\omega\sin\varphi\right) + \frac{\lambda_v + 2\mu_v}{\lambda_e + 2\mu_e}8\omega E - \frac{4\omega^2\rho_0}{\lambda_e + 2\mu_e},$$

$$E = \frac{Ne\rho_0}{4\chi_2}\sin\varphi + \frac{2(\lambda_v + 2\mu_v)\omega^3\rho_0}{(\lambda_e + 2\mu_e)^2 + 4(\lambda_v + 2\mu_v)^2\omega^2},$$

$$H = \frac{1}{R^2 + S^2}\left[(KR + LS) + j(LR - KS)\right],$$

where

$$R = -4\omega^2\rho_0 + 4(\lambda_e + 2\mu_e)(k_1^2 - \alpha_1^2) - 16(\lambda_v + 2\mu_v)\omega k_1\alpha_1 + \frac{\rho_0 Ne}{\chi_2}\left[(\lambda_e + 2\mu_e)\cos\varphi - (\lambda_v + 2\mu_v)2\omega\sin\varphi\right],$$

$$S = -8(\lambda_e + 2\mu_e)k_1\alpha_1 + 8(\lambda_v + 2\mu_v)\omega(k_1^2 - \alpha_1^2) + \frac{\rho_0 Ne}{\chi_2}\left[(\lambda_e + 2\mu_e)\sin\varphi + (\lambda_v + 2\mu_v)2\omega\cos\varphi\right],$$

$$K = -\frac{\rho_0 ND}{\chi_2}[(\lambda_e + 2\mu_e)\cos(2\phi + \varphi) - (\lambda_v + 2\mu_v)2\omega\sin(2\phi + \varphi)],$$

$$L = -\frac{\rho_0 ND}{\chi_2}\left[(\lambda_e + 2\mu_e)\sin\varphi + (\lambda_v + 2\mu_v)2\omega\cos\varphi\right].$$

The parameters of χ_3 and θ used in Eq.(16) are expressed as

$$\chi_3 = \left(X^2 + Y^2\right)^{1/2},$$

$$\theta = \arctan\left(\frac{Y}{X}\right),$$

where

$$X = \frac{2}{R^2 + S^2}\{(KR + LS)\left[\cos(k'x)\exp(-\alpha' x) - 1\right] + (LR - KS)\sin(k'x)\exp(-\alpha' x)\},$$

$$Y = \frac{2}{R^2 + S^2}\{(LR - KS)\left[\cos(k'x)\exp(-\alpha' x) - 1\right] - (KR + LS)\sin(k'x)\exp(-\alpha' x)\},$$

with

$$k' = 2k_1 - k_2, \quad \alpha' = 2\alpha_1 - \alpha_2.$$

References

[1] Gaunaurd G C and Überall H 1978 *J. Acoust. Soc. Am.* **63** 1699

[2] Gaunaurd G C and Überall H 1982 *J. Acoust. Soc. Am.* **71** 282

[3] Gaunaurd G C and Barlow J 1984 *J. Acoust. Soc. Am.* **75** 23

[4] Waterman P C and Truell R 1961 *J. Math. Phys.* **2** 512
[5] Gaunaurd G C and Wertman W 1989 *J. Acoust. Soc. Am.* **85** 541
[6] Ostrovsky L A 1988 *Sov. Phys. Acoust* **34** 523
[7] Ostrovsky L A 1991 *J. Acoust. Soc. Am.* **90** 3332
[8] Toksöz M N and Cheng C H 1980 *J. Acoust. Soc. Am. Supp* **67** S43
[9] Meyer E, Brendel K and Tamm K 1958 *J. Acoust. Soc. Am.* **30** 1116
[10] Qian Z W 1981 *Acta Phys. Sin.* **30** 1 (in Chinese)
[11] Qian Z W 1981 *Acta Phys. Sin.* **30** 10 (in Chinese)
[12] Baird A M, Kerr F H and Townend D J 1999 *J. Acoust. Soc. Am.* **105** 1527
[13] Meulen F V, Feuillard G, Matar O B *et al* 2001 *J. Acoust. Soc. Am.* **110** 2301
[14] Qian Z W, Shao D Y, Li X H *et al* 1999 *Chin. Phys.* **8** 27
[15] Aggelis D G and Tsinopoulos S V and Polyzos D 2004 *J. Acoust. Soc. Am.* **116** 3443
[16] Church C C 1995 *J. Acoust. Soc. Am.* **97** 1510